Digital in-line holography with a divergent beam for 3D velocity field measurement in small volumes

Mokrane Malek, Daniel Allano, Bertrand Lecordier, Frédéric Corbin, Gilles Godard, Denis Lebrun

Digital in-line holography with a divergent beam for 3D velocity field measurement in small volumes

Mokrane Malek[1], Daniel Allano[1], Bertrand Lecordier[1], Frederic Corbin[1], Gilles Godard[1], Denis Lebrun[1]

1: UMR 6614 CORIA, Technopole du Madrillet, 76801 Saint-Etienne du Rouvray, FRANCE

denis.lebrun@coria.fr

Abstract: Digital holography is a well established technique for the study of dynamic volume of particle fields. In this work, an original digital in-line holography system is developed and used to determine 3D displacements of particles tracer in an air-flow. This system allows us to investigate a sample volume of few mm^3 and reconstruct a moving particle with velocities ranging up to $1m.s^{-1}$. The sample volume is reconstructed by computing the wavelet transformation (WT) for different value of the scale parameter. This parameter is related to the axial distance between a reconstruction plane and the CCD sensor. A fiber coupled laser diode is used as the recording light sources. The curvature radius of the reference wave emerging from this fiber forms geometrically magnified diffraction patterns of particles and thus acts as an optical magnification. We show that this enables to enhance the spatial resolution of the system. Here, a transverse magnification ratio of 4 allows us to reconstruct images of droplets with a diameter smaller than 5µm. Note that this configuration needs an accurate knowledge of curvature radius of the recording wave. By using an original calibration method, presented here, we show that the droplets can be localized from the reconstructed holograms with an accuracy of 1µm for lateral position and 20µm in depth. The potential of this system is shown in the case of a laminar air flow seeded with oil micro-droplets.

1. Introduction

Digital in-line holography (DIH) is commonly used to characterize flows seeded by micro-particles. These particles are illuminated with a source of coherent light and the diffraction patterns are directly recorded by CCD camera [Meng *et al*. (2004), Sheng *et al.* (2008), Salah et al. (2008), Malek *et al.* (2008), Cao *et al.* (2007), Garcia-Sucerquia (2006)]. The reconstruction of particle images is often achieved by applying the Fresnel integral to the diffraction patterns [Xu *et al.* (2003), Fournier (2004)] or by using the fractional Fourier transformation [Coëtmellec *et al.* (2003)]. In the case of far-field diffraction, this reconstruction can be seen as a wavelet transform (WT) of the hologram transmission function [Onural (1993)].

The main advantage of DIH is a simple optical arrangement of the recording system composed only by few optical components. This characteristic allows its implementation in several applications, particularly where optical access is difficult. Finally, for more or less all the applications, low-power laser sources such as modulated laser diodes are suitable.

In this paper, we show that DIH can be used to determine 3D velocity fields in small volumes. A diverging reference wave emerges from a fiber coupled laser diode and the curvature radius of the wave leads to a transverse magnification of 4. This configuration allows us to reconstruct images of droplets with a diameter smaller than 5µm and moving with velocities ranging up to 1m/s. The use of divergent beam necessitates an accurate calibration step of the sample volume.

In section 2, the theoretical background used for digital in-line reconstruction of holograms is recalled. In section 3, a description of the proposed method for calibration step is explained. In the same section, an accuracy assessment of this configuration for the axial and transverse localizations is proposed. In the last section, experimental results of 3D particle displacements in air-flow seeded with oil micro-droplets are presented.

2. Theoretical background : Hologram recording with a diverging beam

The principle of the recording in the case of in-line holography is shown in Fig. 1. A coherent light source illuminates an opaque objet of diameter *d* located in the plane (X_e, Y_e) at a distance Z_e from the CCD sensor plane (X',Y'). In the far-field configuration, the distance between the CCD camera and the source light, noted Z_s, can be considered as the curvature radius of the used spherical wave.

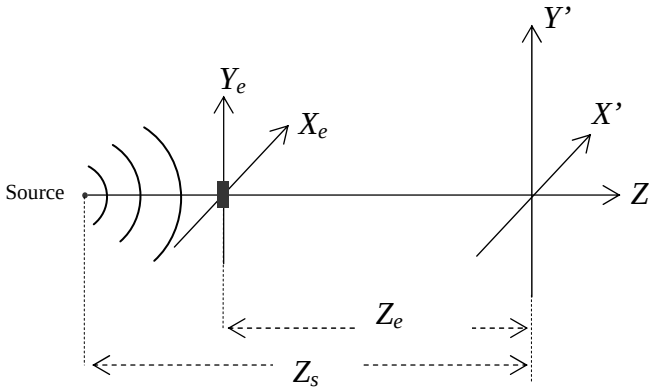

Fig. 1: Optical configuration of recording in-line holograms with a divergent beam.

Under far-field approximation (i.e. $\frac{\pi\left(X_e^{\,2}+Y_e^{\,2}\right)}{\lambda Z_e} << 1$) and by assuming that a spherical wave illuminates the object field, the intensity of the diffraction patterns recorded on the CCD camera at distance Z_e is described by the following expression [Tyler (1976), Vikram (1987)] :

$$I_{Z_{eq}}(X',Y') = 1-\frac{2}{\lambda Z_{eq}}\sin\left(\frac{\pi r^2}{\lambda Z_{eq}}\right)F_{\frac{d_{eq}}{\lambda Z_{eq}}}(r)+\left(\frac{1}{\lambda Z_{eq}}\right)^2 F^2_{\frac{d_{eq}}{\lambda Z_{eq}}}(r) \quad (1)$$

where:

$Z_{eq} = KZ_e$, $d_{eq} = Kd$, $K = \frac{Z_s}{Z_s - Z_e}$, $r^2 = X'^2+Y'^2$ and $F_{\frac{d}{\lambda Z_{eq}}}(r) = \frac{\pi d_{eq}^2}{2}\frac{J_1\left(\frac{\pi d_{eq} r}{\lambda Z_{eq}}\right)}{\frac{\pi d_{eq} r}{\lambda Z_{eq}}}$.

λ is the wavelength and $F_{\frac{d}{\lambda Z_{eq}}}(r)$ is the Fourier transform of the objet transmittance $O(X_e,Y_e)$ at the spatial frequencies $X'/\lambda Z_{eq}$ and $X'/\lambda Z_{eq}$. The object transmittance is

expressed as follows:

$$O(X_e, Y_e) = \begin{cases} 1, & \text{if } \sqrt{X_e{}^2 + Y_e{}^2} \le \dfrac{d}{2}; \\ 0, & \text{otherwise} \end{cases} \tag{2}$$

Note that equation (1) is established by applying the Huygens-Fresnel principle in the scalar diffraction. The first term corresponds to the reference wave; the second describes the interferences between the reference wave and the object diffracted wave. The third term is similar to the diffraction produced by the same aperture as the object. This last term can be neglected in the case of the Fraunhofer approximation [Buraga-Lefebvre (2000)].

The diffraction pattern expressed by the equation (1) shows that the recording by the spherical wave can be modeled as a collimated recording configuration (see Fig. 2). The equivalence between both configurations is obtained by applying a magnification term ($K = \dfrac{Z_s}{Z_s - Z_e}$) to the parameters d and Z_e

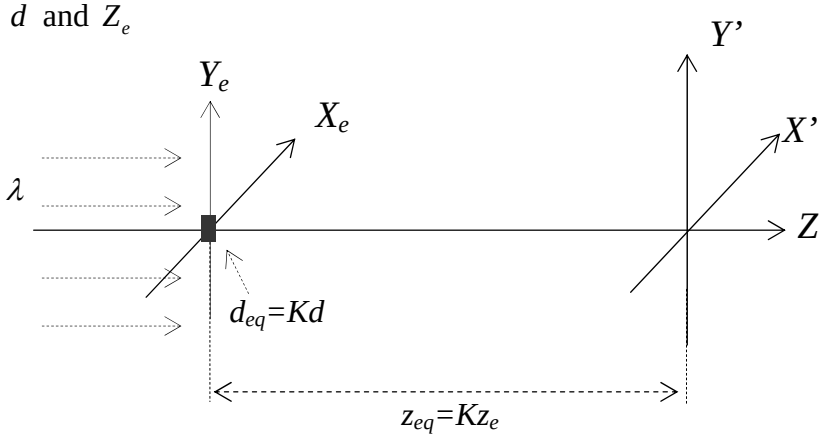

Fig. 2: Hologram recording under Gabor configuration (collimated case): equivalence with the spherical wave configuration showed in Fig. 1.

By this equivalence, the hologram formed by a particle of diameter *d*, illuminated by a divergent wave, and located at a distance Z_e from the CCD sensor, is similar to the hologram generated by a particle of diameter $K \times d$ illuminated by a plane wave and located at a distance $K \times Z_e$ from the CCD.

This interesting result leads to a very simple way for the processing of digital holograms. It means that the diffraction pattern produced by a given object can be processed exactly as if the hologram was recorded with a plane wave and all the conditions of reconstruction (spatial sampling, recording distance, spatial resolution) being expressed in an equivalent magnified space. This principle is illustrated in conventional optical holography representation by Fig. 3.

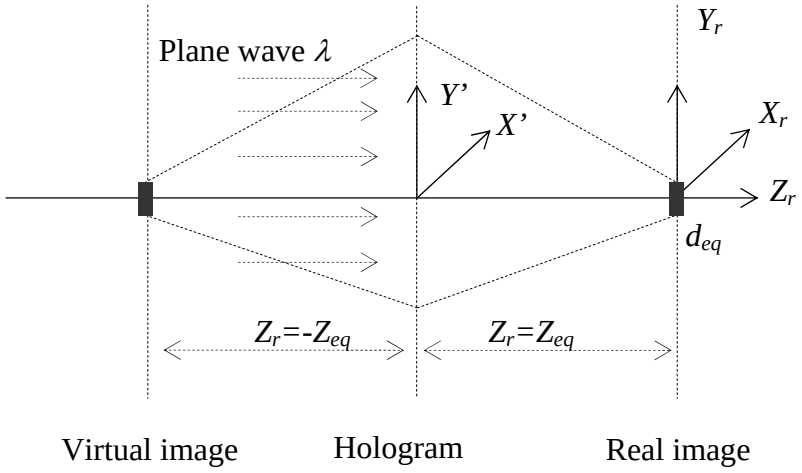

Fig. 3: Digital in-line holography with a spherical recording wave. Equivalent coordinate system under plane wave configuration

As, shown in this figure, the 3D coordinates of a particle image in the reconstruction space are noted here by X_r, Y_r and Z_r.

The following expressions give the relation between the recording (X_e, Y_e, Z_e) and the reconstruction (X_r, Y_r, Z_r) axis systems:

$$\begin{cases} X_e = X_r / K \\ Y_e = Y_r / K \\ Z_e = Z_r / K \end{cases}, \qquad \text{where conjuguate planes lead to: } K = \frac{Z_r + Z_s}{Z_s} \tag{3}$$

In our case, the holograms are reconstructed by a wavelet transform (see Buraga-Lefebvre (2000) for more details). A sample volume is reconstructed plane-by-plane by computing, for different scale parameters, the WT of the recorded diffraction pattern. Each scale parameter of the wavelet is directly related to the axial position Z_r. In the reconstruction space, the axial position of particle image is obtained by the Maximum of the Wavelet Transform Modulus (*MMWT*) according optical axis positions (i.e. Z_r).

3. Calibration method

In practice, the distance between the CCD sensor and the light source (i.e. Z_s) has to be accurately estimated by an appropriate calibration method.

For the calibration, a set of diffraction patterns is recorded from known objects successively localized at different axial positions. Each object position $Z_e^{[i]}$ is adjusted by a micrometer translation stage to a well-defined distance $\Delta Z_e^{[i]}$ centered on the reference plane (Z_{e0}).

The objective of this calibration step is to estimate the value of Z_s by assuming a linear

relation between the measured axial displacements and the calibrated displacements $\Delta Z_e^{[i]}$. This condition gives $Z_e^{[i]}$ = A× $\Delta Z_e^{[i]}$ +B. The estimated value of Z_s is obtained iteratively as described below by a progressive forcing of the parameter A to tend toward 1, and B is an estimated value of Z_{e0}.

In this work the calibration plate is composed of five opaque disks of diameter 10µm deposed on the surface of an optical glass plate. Four disks are placed at the corner of a rectangle of 1mm by 0.7mm, the fifth disk being centered to the others. An example of disk images at reconstructed Z_r = 464.75mm is shown in Fig. 3.a. These images are reconstructed by using the hologram recorded at the reference position. The intensity profiles, according X_r and Z_r coordinates, of the disk noted P5 are respectively shown in Fig. 3 b and Fig. 3 c. These profiles are used to extract the 3D particle images as in [Buraga-Lefebvre (2000)].

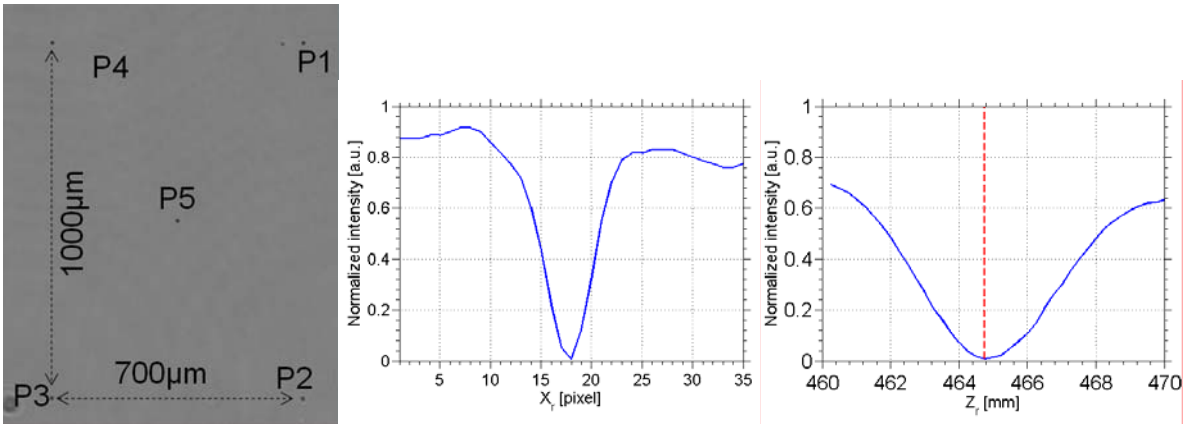

a) b) c)

Fig. 3: a) Example of reconstructed disk images at Z_r=464.75mm. d = 10 µm, b) X_r profile and c) the Z_r profile of disk P5.

For each hologram (i) recorded at a position $Z_e^{[i]} = Z_{e0} + \Delta Z_e^i$, the axial position $Z_r^{[i]}$ of each disk image in the reconstruction space is determined.

Our calibration algorithm estimates iteratively Z_s and Z_{e0}. It uses $\left(Z_r^{[i]}, \Delta Z_e^i\right)$ as input data and works under the following steps:

1) Initialize Z_s by Z_{s0}^0 ;
2) At iteration k and for each displacement $\Delta Z_e^{[i]}$, compute $\hat{Z}_e^{[i]}$ by $\hat{Z}_e^{[i]} = \dfrac{\hat{Z}_{s0} Z_{rj}^{[i]}}{\hat{Z}_{s0} + Z_{rj}^{[i]}}$;
3) Compute the coefficients A and B of the linear regression $\hat{Z}_e^{[i]} = A \times \Delta Z_e^{[i]} + B$
4) Increment the value of $\hat{Z}_{s0} \leftarrow \hat{Z}_{s0} + \Delta Z_s$;
5) Repeat the steps 2, 3 and 4, until $|A - 1| > \varepsilon$.

In this calibration method, ΔZ_s =10^{-3}mm and ε=0.001 have been imposed.

The estimated value of Z_s is obtained after satisfaction of the stop condition (i.e. step 5 of the above algorithm) and a reference axial position (i.e. Z_{e0}) is deduced from the parameter B of

the linear regression.

The Fig. 4 shows the histogram of the measured depth-error δZ_e and *x-y* error (*i.e.*δx and δy) obtained by comparing the measured locations with the imposed *x-y-z* positions. For this experiment, 21 holograms have been recorded and 10 reconstructed images have been processed for each hologram. From these results, the mean square errors are estimated to 7.62µm in depth and to 1.60µm in the *x-y* direction.

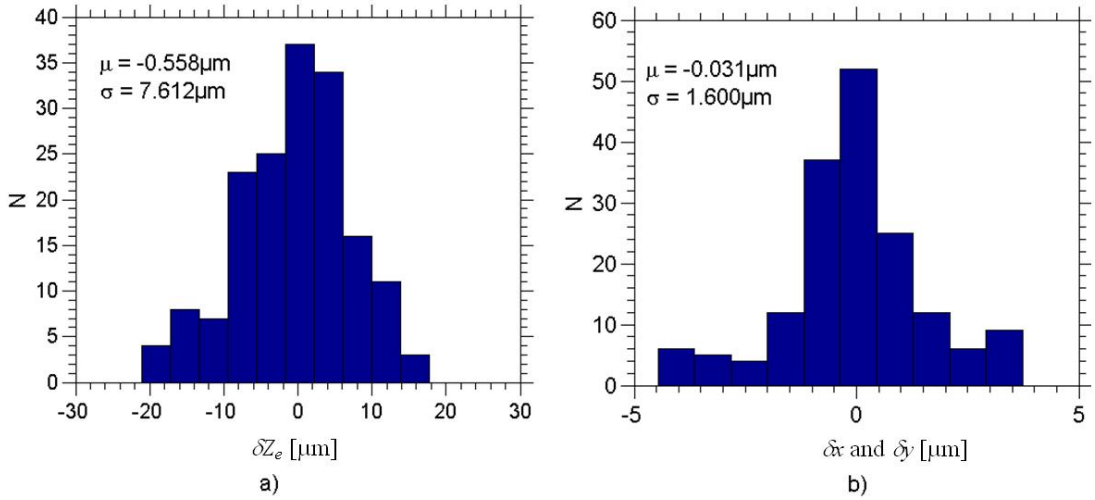

Fig. 4: Estimation of location accuracy by processing 21 holograms of calibrated disks. a) Histograms of depth-error δZ_e and b) transverse error δx and δy computed during the calibration of the experimental setup.

4. Experimental results

4.1. Experimental setup

In the present work, the experimental setup presented in Fig. 5 has been used to validate our DIH system in real experimental conditions. The divergent source light comes from an optical fiber coupled with a modulated laser diode (CUBE 640-25FP) of wavelength λ= 640nm. In continuous mode, this laser delivers a maximum power of 25mW and a TTL signal is used to drive it in pulsed mode. The diffraction patterns are recorded on the interline transfer CCD chip of a Hamamatsu camera (C9300-024). Here, a single frame with a double exposure is used to record the hologram. The size of recorded images is 2048×2048 pixels in 8 bits and the pixel size is equal to 7.4µm. The studied flow is a laminar air jet of 8 mm in diameter (D). This jet, seeded with fine oil droplets in a diameter range between 1 to 5µm, is produced at the outlet port of a porous media. The flow is protected from external environment by a stream of filtered air of 100 mm in diameter in order to avoid any unwanted particles or dust during recording (see Fig. 5). After the reconstruction and 3D localization of particle images, the couples of particle are identified and the displacement of each one is measured.

The first step of the experiment has been to calibrate our recording setup by using the method presented previously in the section 3. The estimated value of the distance between the light source and the CCD sensor is $Z_s = 125$ mm with an optical magnification ranging between 3 and 5. In that configuration, the sample volume of particle field is about 4×4×10 mm^3.

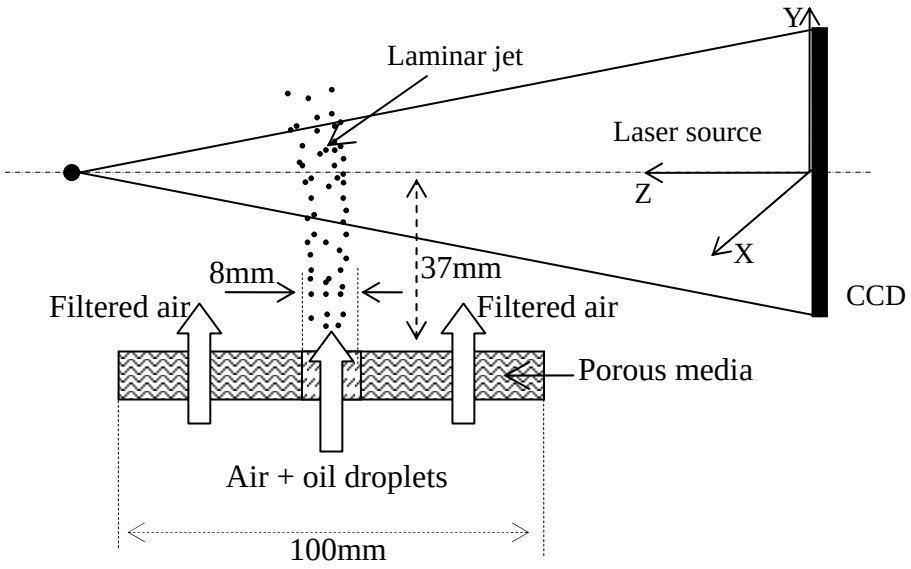

Fig. 5: Recording system with divergent light.

4.2. 3D velocity measurement

In order to validate the potential of our approach for the velocity measurement of small oil droplets, several ten of holograms with different velocity ranges and particle concentration have been recorded. In this experience, the electronic shutter of the CCD camera is set to 110µs to reduce the effect of the background light. The time delay between two laser pulses and pulse duration are respectively equal to 10µs and 1µs. The Figure 6 shows an example of reconstructed image. On a magnification of this image (Fig. 6.b), two couples of particle images are clearly observed and two velocity vectors are then measured.

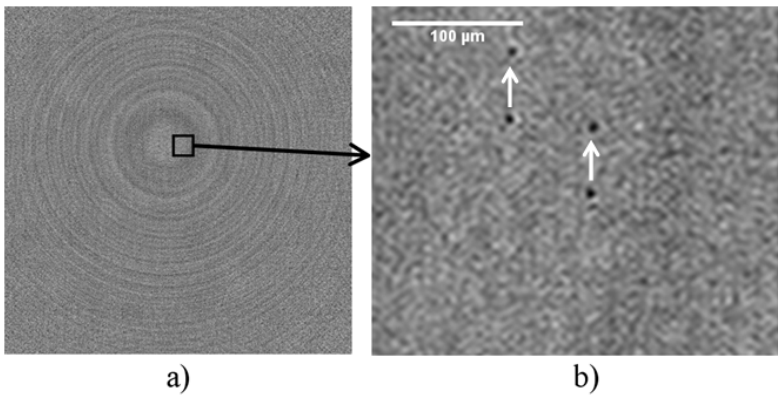

Fig. 6: Example of reconstructed images. Here, particles are located at a distance $Z_e = 98\,mm$ from the camera.

In that experiment, the holograms are used to measure the velocity of droplets along the *Y*-axis versus the axial position (Z_e). The velocity $V_Y / V_{Y\max}$ obtained from four holograms are plotted in Fig. 7 as a function of the axial position Z_e / D. The velocity profile and the axial distance are normalized respectively by the maximum velocity $(V_{Y\max})$ and the jet diameter

(i.e. D = 8mm). The superposition of normalized velocity profiles shows the good reliability of our velocity measurements, obtained in different conditions of velocity and particle concentration.

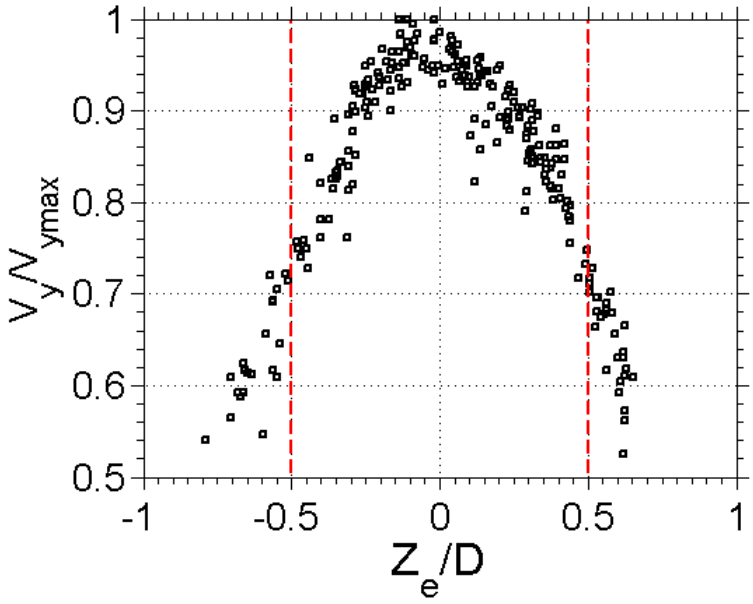

Fig. 7: Evolution of the normalized Y-velocity ($V_Y / V_{Y\max}$) according with normalized axial position (Z_e / D). Here, four holograms are processed.

5. Conclusion

Digital in line holography using a divergent light emerging from a fiber coupled laser diode is well suited for recording holograms of micrometric seeding particles. This capability is obtained by the magnification ratio produced by the curvature radius of the reference wave. The digital reconstruction of particle images by wavelet transform is used to obtain 3D instantaneous spatial distribution of the particle field. This method has been validated in a laminar air jet seeded with oil droplets in the diameter range of 1-5µm and with velocities about 1 m.s^{-1}. It is a significant advance in applications of digital in-line holography in fluid mechanics, where the size of seeding particles is often few pixels in diameter to obtain diffraction patterns with significant visibility. The experimental results obtained in the case of a laminar jet are in good agreement with our expectations and shows the possibilities of this method for instantaneous evaluation of the velocity fields in a sample volume of about 1mm^3.

Acknowledgement:

This work has been supported by the French National Agency (ANR) in the frame of the program : VIVE3D (ANR-07-1188-532) “Vélocimétrie Instantanée Volumique pour les Ecoulements Tridimensionnels".

References

Buraga-Lefebvre C; Coëtmellec S; Lebrun D; Özkul C (2000), Application of wavelet transform to hologram analysis: three-dimensional location of particles, Opt. and Lasers Eng. 33 409-421.

Cao L; Pan G; Woodward S; Meng H (2007), Hybrid digital holography imaging system for 3D Dense Particles field measurement, 7th International Symposium on Particle Image Velocimetry (PIV'07), Rome, Semptember 11-14.

Fournier C; Ducottet C; Fournel T (2004), Digital in-line holography : influence of the reconstruction function on the axial profile of a reconstructed particle image, Meas. Sci. Technol. Vol. 15, p. 686-693.

Garcia-Sucerquia J; Xu W; Jericho S. K; Klages P; Jericho M H; Kreuzer H J (2006), Digital in-line Holographic microscopy, App. Optics, 45, 836-850.

Malek M; Lebrun D; Allano D (2008), Digital in line holography system for threedimensional-three components (3D-3C) Particle Tracking Velocimetry, Eds. A Schröder andC EWiller : Particle Image Velocimetry, Topics Appl. Physics 122, Vol. 15, pp. 157–17.

Meng H; Pan Y; Pu Y; Woodward SH (2004), Holographic particle image velocimetry: from film to digital recording, Meas. Sci. Technol. Vol. 15, p. 673-685

Onural L (1993), Diffraction from a wavelet point of view, Opt. Lett., Vol. 18, p. 846-848.

Salah N; Godard G; Lebrun D; Paranthiën P; Allano D; Coëtmellec S (2008), Application of multiple exposure digital in-line holography to particle tracking in a Bénard-von Kármán vortex flow, Meas. Sci. Technol., Vol. 19, p. 1-7.

Sheng J; Malkiel E; Katz J (2008), Using digital holography microscopy for simultaneous measurements of 3D near wall velocity ans wall shear stress in a turbulent boundary layer, Exp. Fluids, Vol. 45, p. 1023-1035.

Tyler G A; Thompson B J (1976), "Fraunhofer Holography Applied to Particle Size Analysis: A Reassessment," Opt. Acta 23, 685.

Vikram C S; Billet M L (1988), Some salient features if in-line Fraunhofer holography with divergent beams", Optik, 78, 80-83.

Xu W; Jericho M H; and Kreuzer H. J (2003), Tracking particles in four dimensions with in-line holographic microscopy, Opt. Letters, Vol. 28, p. 164-166.